AIAA SciTech Forum
6-10 January 2025, Orlando, FL
AIAA SCITECH 2025 Forum

10.2514/6.2025-1767

Shock-Tube Measurements of NH_2 for Ammonia Kinetics

Matthew Abulail[1] , Claire M. Grégoire[2], Olivier Mathieu[3], and Eric L. Petersen[4]
Texas A&M University, College Station, Texas, 77843, USA

Ammonia is an important molecule in aeronautical and aerospace applications. Current models for ammonia are mostly tuned against ignition delay time, laminar flame speed, and speciation data, yet, there are few data available such as species time histories of intermediates such as NH_2. To assist in resolving ammonia kinetics pathways, an NH_2 diagnostic has been developed at 597.375 nm, based on the known spectroscopy of NH_2. The new diagnostic is utilized with an NH_3 laser stationed at 10440.17 nm to measure species concentration time histories behind reflected shock waves. Using both systems, a 0.008/0.992 NH_3/Ar mixture was tested at 2089 K, 1.27 atm. This paper presents results that demonstrate the successful set up of the absorption diagnostic and its application to a reacting flow field in a shock tube. From the results, an absorption coefficient of 0.8751 cm^{-1}-atm^{-1} was obtained. This method will be applied to acquire a full temperature-dependent absorption coefficient curve for NH_2 and ultimately for monitoring NH_2 in ammonia-based mixtures.

I. Nomenclature

k_v	=	absorption coefficient
P	=	pressure
X_{abs}	=	mole fraction of the measured molecule
L	=	inner diameter of the shock tube
I_0	=	voltage of the signal before crossing the shock tube
I_t	=	voltage of the signal after crossing the shock tube
$\delta_{initial}$	=	voltage offset of the original signal
Δ_{I_0}	=	voltage imbalance of the I_0 photodetector
$\Delta_{I_0-I_t}$	=	voltage imbalance difference between the I_0 and I_t photodetectors
$S(T)$	=	line strength at temperature T
ϕ	=	line shape
$Q(T)$	=	partition function at temperature T
T_0	=	reference temperature (296 K)
T	=	temperature in Kelvins
h	=	Planck's constant
c	=	speed of light
k	=	Boltzmann constant
v_0	=	wavenumber of peak absorption

[1] Graduate Student Researcher, J. Mike Walker '66 Department of Mechanical Engineering, AIAA Student Member
[1] Post Doctorate Researcher, J. Mike Walker '66 Department of Mechanical Engineering, AIAA Member
[3] Research Associate Professor, J. Mike Walker '66 Department of Mechanical Engineering, AIAA Member
[4] Director, TEES Turbomachinery Laboratory, Professor and Nelson-Jackson Chair, J. Mike Walker '66 Department of Mechanical Engineering, AIAA Associate Fellow

v = wavenumber of measuring laser
E'' = lower-state energy for v_0
$N_{L,0}$ = Loschmidt number at 273.15 K
ϕ_V = Voigt line shape
ϕ_G = Gaussian line shape
ϕ_L = Lorentzian line shape
Δv_G = Gaussian full width half maximum of the line shape (FWHM)
M = molecular weight of measured molecule
Δv_L = Lorentzian FWHM
γ_{i-j} = collision parameter between the measuring molecule, i, and the colliding molecule, j
n_j = collisional broadening parameter based on temperature for molecule j
d = dimensionless parameter
C_G = weighted parameter for Gaussian (Doppler) effects
C_L = weighted parameter for Lorentzian (collisional) effects
Δv_v = Voigt FWHM

II. Introduction

Ammonia currently is of interest for power generation as well as to the aeronautical and aerospace industry. Ammonia is a potential replacement for methane, which is important due to the large emphasis on limiting the amount of greenhouse gases released into the atmosphere [1, 2]. Ammonia is constructed with a single nitrogen and three hydrogen atoms, resulting in post-combustion products that exclude a large global warming contributor, carbon dioxide. Additionally, ammonia provides some advantages in terms of production compared to other alternative fuels like hydrogen. Ammonia has a well-defined production process and is easy to store. This set of advantages contributes to the transportation of the fuel as well, thereby making ammonia easier to transport compared to hydrogen [1]. In addition to being a potential replacement for methane, ammonia is also seen in the propellant community since it is an intermediate species in the combustion of many nitrogen-containing propellants. For example, ammonium perchlorate (AP) is an oxidizer comprised of an ammonia molecule connected to perchloric acid. AP exhibits good performance and uniformity with sufficient availability, making it widely used in propellant combustion [3]. With the high dependence on ammonia, a fundamental understanding of ammonia kinetics is necessary to understand the breakdown pathways of ammonia during combustion.

Current models do well at predicting NH_3 decomposition in high-temperature ammonia pyrolysis [4, 5]. Additionally, there have been many studies that provide data for ammonia oxidation and ammonia blends. Past and recent studies have focused on NH_3, N_2O, H_2O, or CO absorption spectroscopy [4-10]. These data are beneficial for validating models; however, current models still struggle to predict many radicals such as NH_2. For example, Fig. 1 presents a comparison of NH_2 time histories obtained from 0-D chemical kinetics simulations (using Chemkin) for four different chemical kinetics models of ammonia combustion. The conditions in Fig. 1 correspond to typical conditions for a reflected-shock experiment for the pyrolysis of NH_3 highly diluted in Ar, at 2000 K and 1 atm. As seen in Fig. 1, there are noticeable differences amongst the predictions from each of the models. Experimental data on NH_2 time histories would provide material for further refinement of ammonia pyrolysis and oxidation at high temperatures.

Therefore, this study employs an NH_2 diagnostic developed at Texas A&M University to help resolve NH_2 chemical kinetics. The system utilizes a laser diode positioned at 8370.7 cm^{-1} at an output power of 160 mW. The laser diode is connected to an HC Photonics frequency doubler to reach 16741.3 cm^{-1} at an output power of ~8mW at a frequency of 501.84 THz. The laser is being employed in conjunction with NH_3 and CO laser absorption diagnostics on the Aerospace Shock Tube at the TEES Turbomachinery Laboratory for simultaneous tracking of multiple

molecules. This paper provides an overview of the operation and post processing of the NH_3 diagnostic, followed by the theory of NH_2 absorption and details the theory for calibrating the new NH_2 diagnostic.

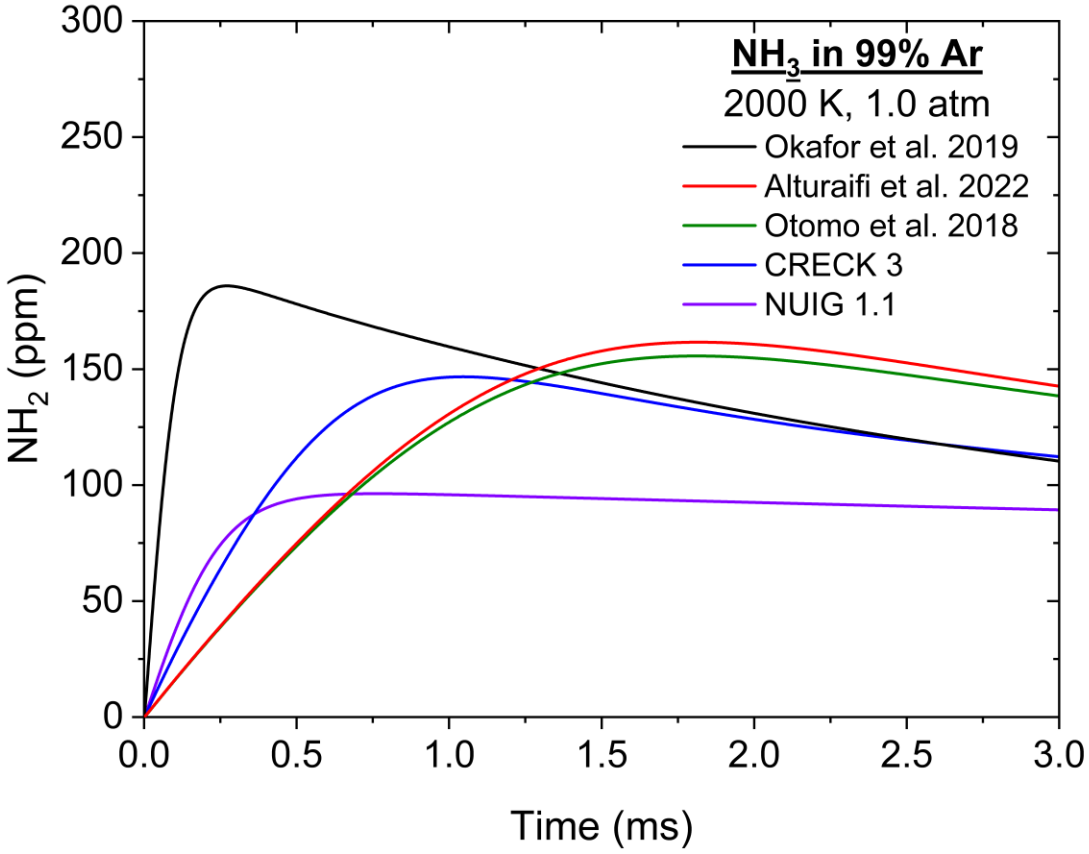

Fig. 1 Calculated NH_2 comparison at 2000 K, 1.0 atm between various chemical kinetics models (Okafor et al. 2019 [4], Alturaifi et al. 2022 [5], CRECK 3 [7], NUIG 1.1 [8], and Otomo et al. 2018 [9]).

III. Methodology

A. Shock-Tube Facilities

The aerospace shock tube (AST) available at Texas A&M University (TAMU) was used for this study. The AST features a driven section with a 16.2-centimeter diameter at 7.88-meters long, and a driver section with a 7.62-centimeter diameter at 3.25-meters long. The AST is a pressure-driven shock tube; that is, it utilizes a pressure difference between the driver and driven section to deform a polycarbonate (Lexan) disc into a sharpened cutter. Upon rupture, an incident wave is produced towards the test mixture, compressing it from the initial temperature and pressure (T_1 and P_1) to the post-incident shock temperature and pressure (T_2 and P_2). When the incident wave reaches the endwall of the driven section, the wave reflects and travels back towards the diaphragm section. This reflected wave further increases the temperature and pressure from T_2 and P_2 to T_5 and P_5. Once the post-reflected shock conditions occur, the test has started.

The AST was chosen specifically for its diagnostic capabilities. First, the AST is made of high-purity stainless steel, which limits the amount of impurities present during chemical kinetics and laser spectroscopy tests. Second, the AST has 5 PCB Piezotronics pressure transducers (model 113A22) placed along the last 1.56 meters before the endwall. Lastly, the AST features 8 ports evenly spaced circumferentially, 1.6 cm from the endwall, thereby allowing for multiple laser, emission, and pressure measurements to occur simultaneously and at the same axial location. For this study, one port houses a sapphire window which transmits light into a focusing mirror and photomultiplier tube to obtain NH_2^* data through a 430 ± 10 nm FWHM narrow bandpass filter. A second port features one of the PCB

pressure transducers to obtain sidewall pressure 1.6 cm from the endwall. The last six ports are a combination of optical window pairs used for laser spectroscopy. A general schematic of this setup is shown in Fig. 2. Currently, NH_3, NH_2, and CO lasers are set up on the AST, but these lasers can easily be interchanged for other laser diagnostics like N_2O and H_2O. This study only be utilized the NH_3 and NH_2 lasers.

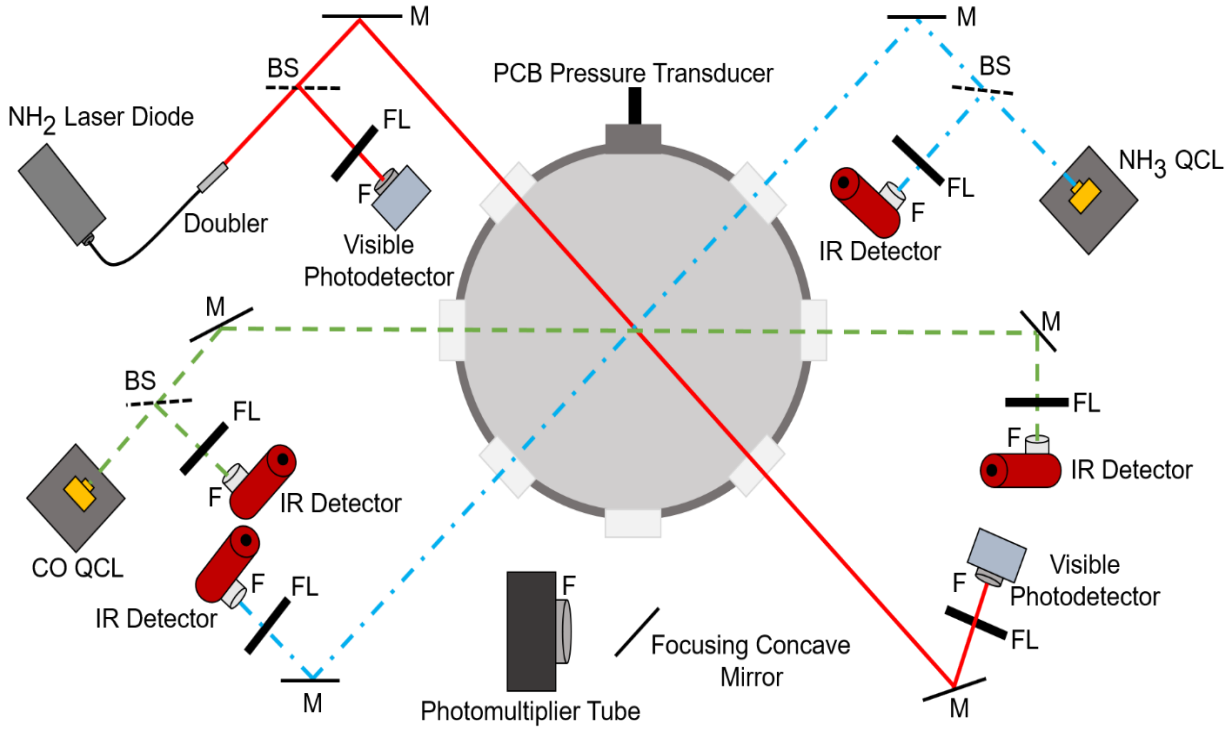

Fig. 2 Schematic of the diagnostic setup on the AST at TAMU, 1.6 cm from the endwall.

B. NH_3 QCL Laser Absorption

As shown by Alturaifi et al. [10,12], direct measurement of the NH_3 concentration within the test section prior to each shock-tube experiment utilizing ammonia as the fuel should be done to compensate for potential adsorption of NH_3 onto the vessel walls. The NH_3 laser diagnostic is shown in Fig. 2. The diagnostic consists of a quantum cascade laser (QCL) operating at 10440.17 nm (957.839 cm^{-1}), which produces ~27 mW of power at 31.1°C. The absorption of NH_3 is measured by sending the QCL laser through a 50/50 beam splitter, with one end being the baseline (or incident) signal, and the other beam being sent through the shock tube (transmitted signal). Both beams enter into separate IR photodetectors, where both signals are recorded at a rate of 1 million samples a second. These signals are then used in the Beer-Lambert relationship shown in Eq.1. Note, Eq.1 does not account for any offsets or imbalances resulting from the photodetectors. To account for detector offsets, Mulvihill created the relationship shown in Eq. 2 to account for these biases [11]. These imbalances do not scale the signals, but rather just shift the lines, thereby making the signals true. Mulvihill witnessed a 4.2% error when neglecting to include this in his processing results, therefore emphasizing the necessity of Eq. 2 [11].

$$\ln\left(\frac{I_t}{I_0}\right) = -k_v P X_{abs} L \tag{1}$$

$$\frac{I_t}{I_0} = 1 - ((I_0 - I_t)_{measured} - \delta_{initial})/(((I_0)_{measured} - \Delta_{I_0}) - (\delta_{initial} - \Delta_{I_0 - I_t})) \tag{2}$$

During an experiment, the raw signals of the photodetectors, the pressure, and the inner diameter of the AST are known. Additionally, the deltas present in Eq. 2 are obtained before and after each test, therefore leaving the absorption coefficient in Eq. 1 the only unknown needed to solve for the mole fraction of ammonia. NH_3 absorption at this wavelength is well known, with HITRAN and Alturaifi et al. providing key parameters such as line strength and collisional parameters [12, 13]. The absorption coefficient can be written as the product of the line strength and the line shape. The line strength is calculated in Eq. 4, where the line strength at T_0 is simply multiplied by a scalar. Q and E" for 957.839 cm^{-1} are both available in HITRAN [13]. Using this definition of line strength requires modifying the absorption coefficient in Eq. 3 to the definition seen in Eq. 5. This revision includes the Loschmidt number, which converts the line strength units from cm-molecule^{-1} to cm^{-2}-atm^{-1} and the Voigt line shape. The Loschmidt number is 2.6867811×10^{19} molecules per cm^3 at 273.15 K. A temperature term is also included in Eq. 5 to account for the effect of changing temperature on the Loschmidt number.

$$k_v = S(T)\phi \tag{3}$$

$$S(T) = S(T_0)\frac{Q(T_0)}{Q(T)}\exp\left(-\frac{hcE''}{k}\left(\frac{1}{T}-\frac{1}{T_0}\right)\right)\left(1-\exp\left(\frac{-hc\nu_0}{kT}\right)\right)\left(1-\exp\left(\frac{-hc\nu_0}{kT_0}\right)\right)^{-1} \tag{4}$$

$$k_v = N_{L,0}\left(\frac{273.15}{T}\right)S(T)\phi_V \tag{5}$$

Replacing the absorption coefficient with the line strength requires some knowledge of the line shape. To best model the line shape, a convolution of a Gaussian and Lorentzian profile, often referred to as the Voigt profile, can be used. The Gaussian portion incorporates the thermal motion of the molecule (Doppler broadening), while the Lorentzian profile accounts for the collisional effects of the molecule. The common definition for the Voigt profile is give in Eq. 6. Calculating a convolution of the Gaussian and Lorentzian profiles for subtle changes in temperature and pressure is computationally intensive. Liu et al. has calculated a simplification of the Voigt profile by utilizing the Gaussian and Lorentzian full width half maximum (FWHM) shown in Eqs. 7 and 8 [14]. The FWHMs are based on the molecular weight of the molecule, the wavenumber, the initial mole fractions of the mixture, post-reflected shock temperature and pressure (T_5 and P_5), and the collisional parameter. The collision parameter is determined experimentally and is calculated for the measured molecule, i (in this case is NH_3), and the colliding molecule, j, which are the other molecules in the mixture at the reference temperature. The collisional parameter is multiplied by a temperature correction which utilizes a collision broadening variable, n_j, to properly scale the collisional parameter to different temperatures.

$$\phi_V = \phi_G \times \phi_L \tag{6}$$

$$\Delta\nu_G = 7.162E-7 * \nu_0\sqrt{T/M} \tag{7}$$

$$\Delta\nu_L = 2P\sum_j X_j\gamma_{i-j}(T_0) \tag{8}$$

$$\gamma_{i-j}(T) = \gamma_{i-j}(T_0)\left(\frac{T_0}{T}\right)^{n_j} \tag{9}$$

The pseudo-Voigt profile takes the Gaussian and Lorentzian FWHMs and constructs a dimensionless parameter d, shown in Eq. 10. The parameter d is then used in Eqs. 11 and 12 to create two weighted coefficients (C_G and C_L). Additionally, Eq. 13 shows the pseudo-Voigt FWHM parameter which is calculated using a combination of the Gaussian and Lorentzian FWHMs. Utilizing the weighted coefficients, the pseudo-Voigt FWHM, and the wavenumber, the Voigt line shape is estimated as shown in Eq. 14 [14].

$$d = (\Delta\nu_G - \Delta\nu_L)/(\Delta\nu_G + \Delta\nu_L) \tag{10}$$

$$C_G = 0.68188 + 0.61293 * d - 0.18384 * d^2 - 0.11568 * d^3 \tag{11}$$

$$C_L = 0.32460 - 0.61825 * d + 0.17681 * d^2 + 0.12109 * d^3 \tag{12}$$

$$\Delta v_v = \sqrt{\Delta {v_L}^2 + \Delta {v_G}^2 / ln(2)} \tag{13}$$

$$\phi_v = \frac{C_L}{\pi} \frac{\Delta v_v}{(v-v_0)^2 + \Delta {v_v}^2} + \frac{C_G \sqrt{\ln(2)}}{\Delta v_v \sqrt{\pi}} \exp\left(\frac{-\ln(2)(v-v_0)^2}{\Delta {v_v}^2}\right) \tag{14}$$

C. NH_2 Laser Setup

Ideally, NH_2 measurements would be processed in a similar fashion as NH_3, however the full spectra absorption of NH_2 is relatively unknown. In addition to the relatively unknown absorption bands of NH_2, it is an intermediate radical (NH_2 needs to be produced to be measured). Thankfully, there have been a few key studies in the past which have measured NH_2 absorption in the visible wavelength region. Dressler and Ramsay detailed the electron absorption spectra of NH_2 between 513.5 to 630 nm in 1959 [15]. Although the uncertainty was high, Dressler and Ramsay set up the study done by Sandia National Laboratory which refined the spectra data between 597.1 to 603.3 nm. In the same report, Sandia also investigated relative NH_2 concentrations in a burner back in 1981 [16]. Sandia used a wavenumber of 16739.9 cm^{-1} for their study as it showed the highest absorbance in the 597.1 to 603.3 nm band. It would not be until 1988 when Kohse-Höinghaus et al. utilized the same absorption band to create an NH_2 diagnostic for ammonia pyrolysis in a shock tube. The findings from Kohse-Höinghaust et al. were used within the same research group in Davidson et al. provide the only NH_2 spectroscopic data for ammonia pyrolysis [17, 18]. Nearly a decade later, Votsmeier et al. would revisit the study by Kohse-Höinghaus et al. and revise the absorption coefficient, which was estimated to be off by 30% in the lower-temperature region of 1600-2000 K [19].

Therefore, a new NH_2 diagnostic has been developed at Texas A&M University to obtain NH_2 Chemical spectroscopy data. The new diagnostic is based on a MOGLabs tunable diode laser (TDL) producing 420 mW of power at 1197.75 nm. The output of the TDL enters a fiber coupler which transmits the laser light into a HC Photonics waveguide mixer. The waveguide mixer takes the incoming signal at 1197.75 nm and 420 mW and outputs the beam at 597.375 nm at 8.7 mW. Similar to the NH_3 laser diagnostic, the beam is split through a 50/50 beam splitter, with one beam traversing the shock tube into a photodetector, I_t, and the other beam directed into a separate photodetector as the control, I_0.

As mentioned before, many of the variables for NH_2 are unknown. Green and Miller used relative signals to get around this issue, while Kohse-Höinghaus et al. and Votsmeier et al. defined an NH_2 absorption coefficient based on a compiled chemical kinetic model [16, 17, 19]. Traditionally, both methods are seen as unfavorable since relative signals do not provide any information of the concentration, and chemical kinetic models could be seen as unreliable depending on the molecule and the size of the mechanism. This means that if a chemical mechanism was used, it would have to be well reviewed and thoroughly validated. Alturaifi et al. has done just that with his mechanism on NH_3 pyrolysis. Not only is it a full mechanism, it is tuned based on NH_3 traces taken with the same NH_3 diagnostic in section 2.B. This mechanism has a high accuracy in NH_3 chemistry, but the accuracy of the NH_2 chemistry is unknown. As a result, a similar procedure to Kohse-Höinghaust et al. is taken, where there is a limit to the amount of time the model and the raw signals are correlated. For the case of Kohse-Höinghaus et al., the limit is based on a linear region apparent in the first 50 μs of the signal, with the maximum calibration time being around 50-60 μs [17]. This technique would be ideal for lower-temperature cases, where the decomposition of NH_2 would take longer than 50 μs before occurring; however, the uncertainty at higher temperatures would make this method unrealistic. To improve the method to provide more reliable results, a sensitivity analysis was run at each condition. The time at which the summation of all NH_2-consuming reactions equal 5% is determined to be the maximum correlation time. This criterion is an arbitrary value chosen by the decrease seen in the linearity of the NH_2 concentration. Therefore, the chosen result is to process the data using Eqs. 1 and 2, and using the Alturaifi et al. NH_3 pyrolysis model to correlate the model to the signal for the time specified in the sensitivity analysis.

IV. Results

A 0.008/0.992 NH_3/Ar mixture is made for this experiment. The mixture composition is similar to that of Davidson et al. for comparison purposes to the previous NH_2 study [18]. Figure 3 depicts the sensitivity analysis for ammonia pyrolysis at conditions of 2089 K and 1.27 atm. The production of NH_2 occurs very rapidly, with the $NH_3 + M \rightarrow NH_2 + H + M$ and $NH_3 + H_2 \rightarrow NH_2 + H$ reactions being the only two NH_2 production pathways. With NH_3 pyrolysis kinetics being well refined within the Alturaifi et al. model, therefore reinforcing that NH_2 concentrations are accurate prior to the destruction of NH_2. As such, using the calibration methodology stated in section III.C, the conditions below have approximately 33 μs of test time for calibrating the NH_2 absorption coefficient.

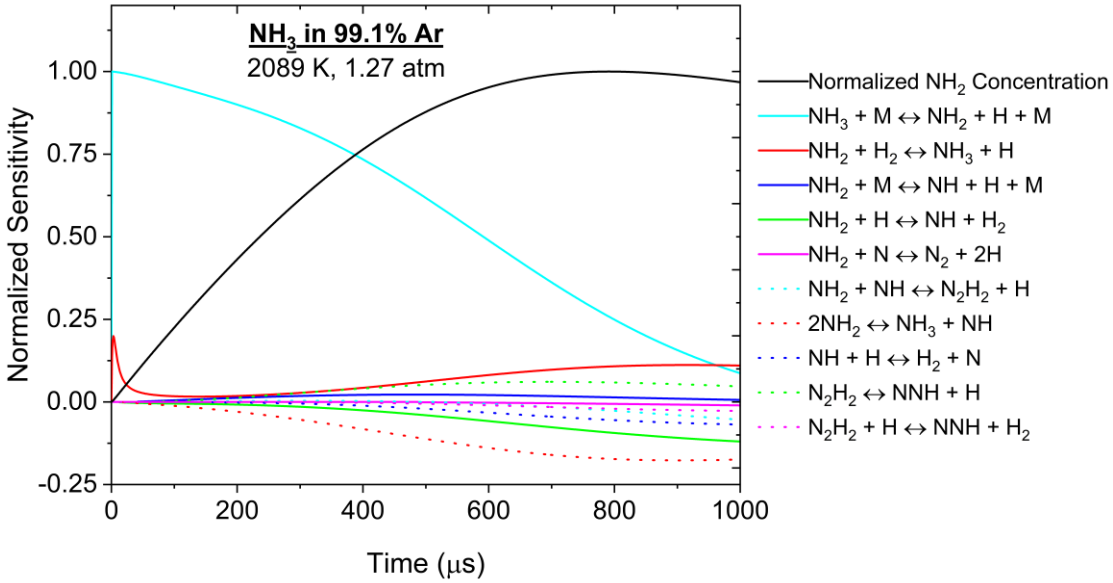

Fig. 3 Sensitivity analysis of NH_2 using Alturaifi et al. at 2089 K, 1.27 atm.

The same conditions shown in Fig. 3 were taken using the NH_3 and NH_2 diagnostics in the AST, and the results are presented in Figs. 4 and 5. Before each test, 10 torr of the test mixture was inserted into the shock tube. This initial amount of ammonia is used to passivate the stainless steel. The mixture was left for 10 mins before being vacuumed to 1 torr, after which the driven section was filled to the initial desired pre-test driven pressure. Passivation prevents ammonia from adsorbing onto the stainless steel by saturating the stainless steel prior to a test. However, over passivation can occur, where the ammonia adsorbed into the stainless steel after passivation can be re-released into the pre-test mixture prior to (or during) an experiment. Thankfully, a NH_3 diagnostic was available for correcting initial concentration issues at lower temperatures, but this correction is difficult to do at higher temperatures since NH_3 pyrolysis occurs too quickly to verify the initial amount of NH_3 after reflected-shock arrival.

Currently, an additional study is being performed by the authors to further investigate and minimize this interference effect, but since 2089 K is a low enough temperature, the amount of ammonia that leaked is calculated to be around 950 ppm higher than the original mixture (or about 10% of the original NH_3). The sensitivity analysis in Fig. 3 has accounted for this effect. Additionally, the ammonia pyrolysis model from Alturaifi et al. [5] was run for both the initial and over passivation concentrations shown in Fig. 4. The higher-NH_3 concentration model was used for estimating the NH_2 for the calibration. The test shown herein is, thus, mainly for demonstration purposes. Once the over-passivation issue is minimized, a thorough NH_2 absorption coefficient calibration study can be conducted.

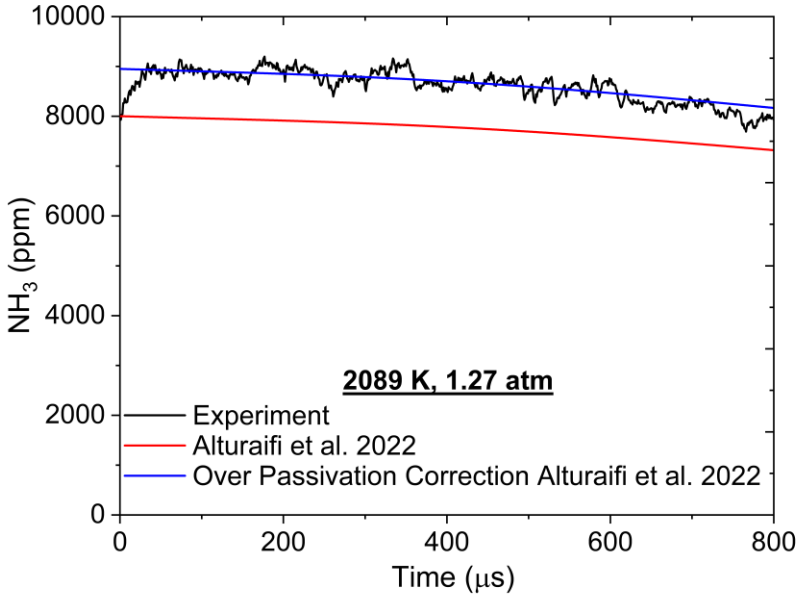

Fig. 4 NH_3 concentration time history at 2089 K, 1.27 atm showing the correction for over-passivation in the experiment.

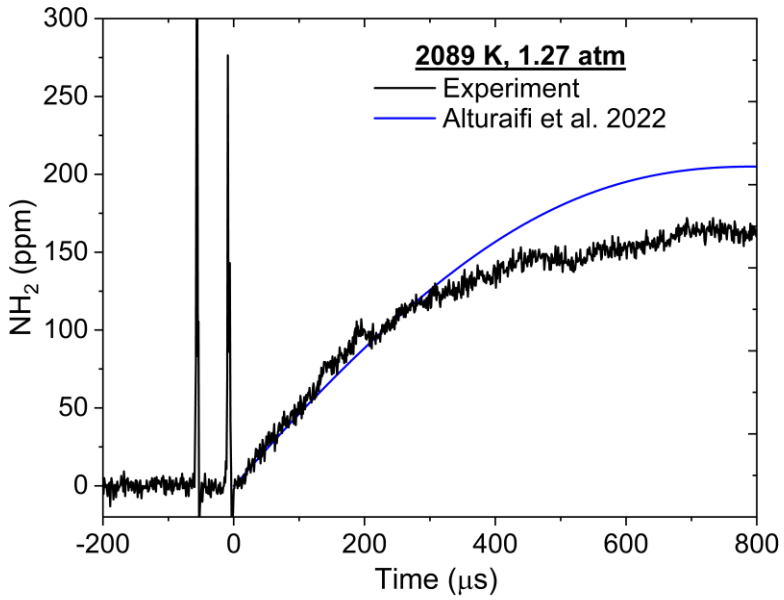

Fig. 5 Measured NH_2 concentration time history at 2089 K, 1.27 atm.

NH_3 results show good correlation with the results from the Alturaifi et al. model, as expected, particularly at earlier times (Fig. 5). The NH_2 result is use to calibrate the absorption coefficient with the first 33 μs, and the obtained absorption coefficient is 0.8751 cm^{-1}-atm^{-1}. At similar conditions, Kohse-Höinghaus et al. predicts the absorption coefficient to be 3.161 cm^{-1}-atm^{-1} [17]. As shown in Fig. 5, NH_2 displays a peak lower than that of Alturaifi et al. [5]. However, the Alturaifi et al. model was calibrated to the peak NH_2 ppm values obtained from Davidson et al. Note, the NH_2 peak ppm values by Davidson et al. were taken in a temperature region between 2000 and 3200 K and used the absorption coefficients from Kohse-Höinghaust et al., not the correction by Votsmeier et al. This new measurement of the absorption coefficient presents some issue with the previous study by Davidson et al., since ammonia models significantly improved since the initial study from Kohse-Höinghaust et al., and the absorption coefficient at lower temperatures (1600 - 1950 K) showed a near 30% deviation from the original study, according to the follow up study

from Votsmeier et al., hence implying the absorption coefficient might also deviate in the higher-temperature region [19]. Additionally, NH_3 was not tracked during the literature experiments, and no passivation was applied before testing, so the peak NH_2 concentrations present in Davidson et al. [5, 17, 18] should be revisited with more experiments using the present setup.

Based on the methodology outlined in this paper, the next steps regarding the NH_2 diagnostic are to comlete an absorption curve and create a comparison between the data provided in Davidson et al. Upon completion, other key studies such as ammonia oxidation and ammonia-hydrogen mixtures can be studied using the new NH_2 setup.

V. Conclusion

A NH_2 laser absorption diagnostic was developed and tested to assist in resolving ammonia kinetics by providing temporal concentrations of NH_2 during NH_3 pyrolysis. Additionally, an NH_3 laser setup previously demonstrated in the authors' laboratory was used along with the NH_2 diagnostic. NH_3 and NH_2 laser absorption measurements were taken at 2089 K and 1.27 atm behind the reflected shock wave. Per the sensitivity analysis from the Alturaifi et al. model at the relevant conditions, the NH_2 absorption coefficient was calibrated using the first 33 μs of the data, resulting in an absorption coefficient of 0.8751 cm^{-1}-atm^{-1} at 2089 K. Future plans for the new NH_2 diagnostic are to continue obtaining absorption coefficients for a wide variety of temperatures and construct an absorption coefficient curve.

Acknowledgments

Funding for this work was provided in part by the National Science Foundation, Grant number 2308433.

References

[1] Kobayashi, H., Hayakawa, A., Somarathne, K. D. K. A., and Okafor, E. C., "Science and Technology of Ammonia Combustion," *Proceedings from the Combustion Institute*, Vol. 37, 2019, pp. 109-133.

[2] Zhu, Y., Curran, H. J., Girhe, S., Murakami, Y., Pitsch, H., Senecal, K., Yang, L., and Zhou, C.-W., "The Combustion Chemistry of Ammonia and Ammonia/Hydrogen Mixtures: A Comprehensive Chemical Kinetic Modeling Study," *Combustion and Flame*, Vol. 260, 2024, pp. 113239.

[3] Sutton, G. P., and Biblarz, O., *Rocket Propulsion Elements*, 9th ed., Wiley, New Jersey, 2017, pp. 513-515.

[4] Okafor, E. C., Naito, Y., Colson, S., Ichikawa, A., Kudo, T., Hayakawa, A., and Kobayashi, H., "Measurement and Modelling of the Laminar Burning Velocity of Methane-Ammonia-Air Flames at High Pressures Using a Reduced Reaction Mechanism," *Combustion and Flame*, Vol. 204, 2019, pp. 162-175.

[5] Alturaifi, S. A., Mathieu, O., and Petersen, E. L., "An Experimental and Modeling Study of Ammonia Pyrolysis," *Combustion and Flame*, Vol. 235, No. 111694, 2022.

[6] Stagni, A., Arunthanayothin, S., Dehue, M., Herbinet, O., Battin-Leclerc, F., Bréquigny, P., Mounaïim-Rouseselle, C., and Faravelli, T., "Low-and Intermediate-Temperature Ammonia/Hydrogen Oxidation in a Flow Reactor: Experiments and a Wide-Range Kinetic Modeling," *Chemical Engineering Journal*, Vol. 471, No.144577, 2023.

[7] Stagni, A., Cavallotti, C., Arunthanayothin, S., Song, Y., Herbinet, O., Battin-Leclerc, F., and Faravelli, T., "An Experimental, Theoretical and Kinetic-Modeling Study of the Gas-Phase Oxidation of Ammonia," *Reaction Chemistry & Engineering*, Vol. 5, 2020, pp. 696-711.

[8] Dong, S., Wang, B., Jiang, Z., Li, Y., Gao, W., Wang, Z., Cheng, X., and Curran, H. J., "An Experimental and Kinetic Modeling Study of Ammonia/n-Heptane Blends," *Combustion and Flame*, Vol. 246, No. 112428, 2020.

[9] Otomo, J., Koshi, M., Mitsumori, T., Iwasaki, H., and Yamada, K., "Chemical Kinetic Modeling of Ammonia Oxidation with Improved Reaction Mechanism for Ammonia/Air and Ammonia/Hydrogen/Air Combustion," *International Journal of Hydrogen Energy*, Vol. 43, No. 5, 2018, pp. 3004-3014.

[10] Alturaifi, S. A., Mathieu, O., and Petersen, E. L., "A Shock-Tube Study of NH_3 and NH_3/H_2 Oxidation Using Laser Absorption of NH_3 and H_2O," *Proceedings from the Combustion Institute*, Vol. 39, 2023, pp. 233-241.

[11] Mulvihill, C. R, "H_2O Laser Absorption and OH* Chemiluminescence Measurements of H_2-NO_2 Oxidation in a Shock Tube," Ph. D Dissertation, J. Mike Walker '66 Department of Mechanical Engineering, Texas A&M University, College Station, Texas, USA, 2019.

[12] Alturaifi, S. A., and Petersen, E. L., "Ammonia Line Strengths and N_2-, O_2-, Ar-, He-, and Self-Broadening Coefficients in the v_2 Band Near 10.4 μm," *Journal of Quantitative Spectroscopy and Radiative Transfer*, Vol. 262, 2021, pp. 107516.

[13] Rothman, L. S., Barbe, A., Benner, D. C., Brown, L. R., Camy-Peyret, C., Carleer, M. R., Chance, K., Clerbaux, C., Dana, V., Devi, V. M., Fayt, A., Flaud, J.-M., Gamache, R. R., Goldman, A., Jacquemart, D., Jucks, K.W., Lafferty, W. J., Mandin, J.-Y., Massie, S. T., Nemtchinov, V., Newnham, D. A., Perrin, A., Rinsland, C. P., Schroeder, J., Smith, K. M., Smith, M. A. H., Tang, K., Toth, R. A., Vander Auwera, J., Varanasi, P., and Yoshino, K., "The HITRAN Molecular Spectroscopic Database:

Edition of 2000 Including Updates Through 2001," *Journal of Quantitative Spectroscopy and Radiative Transfer*, Vol. 82, No. 1-4, 2003, pp. 5-44.
[14] Liu, Y., Lin, J., Huang, G., Guo, Y., and Duan, C., "Simple Empirical Analytical Approximation to the Voigt Profile," *Journal of the Optical Society of America B*, Vol. 18, No.5, 2001, pp. 666-672.
[15] Dressler, K., and Ramsay, D. A., "The Electronic Absorption Spectra of NH_3 and ND_2," *Philosophical Transactions of the Royal Society of London, Series A: Mathematical, Physical and Engineering Sciences*, Vol. 251, 1959, pp. 553-604.
[16] Green, R. M., and Miller, J. A., "The Measurements of Relative Concentration Profiles of NH_2 Using Laser Absorption Spectroscopy," SAND80-8858, Albuquerque, New Mexico, January 1981.
[17] Kohse-Höinghaus, K., Davidson, D. F., Chang, A. Y., and Hanson, R. K., "Quantitative NH_2 Concentration Determination in Shock Tube Laser-Absorption Experiments," *Journal of Quantitative Spectroscopy and Radiative Transfer*, Vol. 42, 1989, pp. 1-17.
[18] Davidson, D. F., Kohse-Höinghaus, K., Chang, A. Y., and Hanson, R. K., "A Pyrolysis Mechanism for Ammonia," *International Journal of Chemical Kinetics*, Vol. 22, 1990, pp. 513-535.
[19] Votsmeier, M., Song, S., Davidson, D. F., and Hanson, R. K., "Shock Tube Study of Monomethylamine Thermal Decomposition and NH_2 High Temperature Absorption Coefficient," *International Journal of Chemical Kinetics*, Vol. 31, No. 5, 1999, pp. 323-330.